Electronic Supplementary Information

Twisted D-π-A solid emitters: efficient emission and high contrast mechanochromism

Yongyang Gong,[a] Yeqiang Tan,[b] Jun Liu,[c] Ping Lu,[d] Cunfang Feng,[d] Wang Zhang Yuan,*[a] Yawei Lu,[a] Jing Zhi Sun,[b] Gufeng He*[b] and Yongming Zhang*[a]

[a] *School of Chemistry and Chemical Engineering, Shanghai Jiao Tong University, Shanghai 200240, China*
Email: wzhyuan@sjtu.edu.cn (W.Z.Y.), ymzsjtu@yahoo.com.cn (Y.Z.). Fax: +86-21-54742567, Tel: +86-21-34202613.
[b] *Department of Polymer Science and Engineering, Zhejiang University, Hangzhou 310027, China*
[c] *National Engineering Lab for TFT-LCD Materials and Technologies, Department of Electronic Engineering, Shanghai Jiao Tong University, Shanghai 200240, China*
Email: gufenghe@sjtu.edu.cn (G.H.)
[d] *State Key Lab of Supramolecular Structure and Materials, Jilin University, Changchun 130012, China*

Table of Content

Fig. S9 ^{13}C NMR spectrum of PhNPATPAN.

Fig. S10 Normalized absorption spectra of DPATPAN, MeDPATPAN and PhNPATPAN in THF.

Fig. S11 Normalized (A) absorption and (B) emission spectra of DPATPAN in varying solvents. Excitation wavelength = 380 nm. Concentration: 20 μM.

Fig. S12 Photographs of DPATPAN in different solvents under (left) room light and (right) 365-nm UV light illumination. Concentration: 20 μM.

Fig. S13 (A) PL spectra of MeDPATPAN in THF and THF/water mixtures with varying water fractions (f_w). (B) Plot of PL intensity of MeDPATPAN at 547 nm *vs* f_w. Concentration: 10 μM; excitation wavelength: 400 nm. Photographs in (B) are MeDPATPAN in THF and 10/90 THF/water mixture taken under 365-nm UV light illumination.

Fig. S14 (A) PL spectra of PhNPATPAN in THF and THF/water mixtures with varying water fractions (f_w). (B) Plot of PL peak intensity of PhNPATPAN *vs* f_w. Concentration: 10 μM; excitation wavelength: 400 nm. Photographs in (B) are PhNPATPAN in THF and 10/90 THF/water mixture taken under 365-nm UV light illumination.

Fig. S15 Photographs of DPATPAN dotted on a TLC plate placed in air under (A) room light and (B) 365-nm UV light and in (C) DCM, (D) chloroform, and (E) THF vapors under 365-nm UV light irradiation.

Fig. S16 Emission maxima of DPATPAN during the grinding-heating cycles. As = as prepared sample, G = ground sample; An = annealed sample (annealed at 80 ^{o}C for 10 min). The numbers after G or An represent cycle numbers.

Fig. S17 (A, B) Emission spectra and (C, D) photographs (under 365-nm UV light irradiation) of as prepared and ground solids for (A, C) MeDPATPAN and (B, D) PhNPATPAN, respectively.

Fig. S18 (A, B) ORTEP drawings and (C, D) molecular packing of the crystals for (A, C) MeDPATPAN and (B, D) PhNPATPAN-NP, respectively. Exampled C−H···N and C−H···π intermolecular interactions are depicted in B and D.

Fig. S19 B3LYP/6-31G(d) calculated molecular orbital amplitude plots of HOMO and LUMO levels for MeDPATPAN and PhNPATPAN.

Fig. S20 (A) EL spectra of DPATPAN, MeDPATPAN and PhNPATPAN with the device configuration of ITO/NPB (60 nm)/X (30 nm)/Alq_3 (30 nm)/Liq (1 nm)/Al (150 nm), (B) plots of luminance-voltage-current density, (C) plots of current efficiency and power efficiency *versus* driving voltage of the devices, and (D) external quantum efficiency as a function of the luminance.

Fig. S21 (A) Emission spectra of vacuum deposited thin films of DPATPAN, MeDPATPAN andPhNPATPAN and (B) their photographs taken under 365-nm UV light illumination.

Experimental Section

Materials. Benzophenone (**1**) and 4-bromophenylacetonitrile (**2**) were obtained from J&K Chemical Scientific Ltd. Sodium tert-butoxide, sodium hydride, palladium diacetate, diphenylamine, 4-methyldiphenylamine and *N*-phenyl-1-naphthylamine were obtained from TCI. Tri-*tert*-butylphosphine (0.5 M in toluene) was purchased from Puyang Huicheng Electronic Material Co., Ltd (China). Benzene, dichloromethane (DCM) and toluene were distilled under normal pressure from CaH_2 under nitrogen immediately prior to use. THF was distilled from sodium/benzophenone under nitrogen before use. Other commercially available reagents were used without further purification.

Instruments. ^{1}H NMR (400 MHz) and ^{13}C NMR (100 MHz) spectra were recorded on a Bruker AMX-400 NMR spectrometer in deuterated solvent at room temperature, and chemical shifts were reported in ppm relative to tetramethylsilane (TMS). Mass spectra were recorded on a Varian 500-MS ion trap mass spectrometer with APCI ion source. UV-vis absorption and emission measurements were performed on a TU-1901 UV-vis spectrophotometer and a Perkin-Elmer LS 55 fluorospectrometer, respectively. Emission quantum yields of the luminogens in solvents were estimated by using quinine sulfate as standard, while solid-state efficiencies were determined using a PTI C-701 calibrated integrating sphere (4 in) with the excitation wavelength of 325 nm. The ground-state geometries were optimized using the density functional with B3LYP hybrid functional at the basis set level of 6-31G(d). All calculations were performed using the Gaussian 09 package.

Single-crystal X-ray diffraction intensity data were collected on a Bruker–Nonices Smart Apex CCD diffractometer with graphite-monochromated Mo-Ka radiation. Processing of the intensity data was carried out using the SAINT and SADABS routines, and the structure and refinement were conducted using the SHELTL suite of X-ray programs (version 6.10).

Preparation of aggregates: A stock solution of samples in THF with a concentration of 100 μM was prepared. An aliquot (1 mL) of the stock solution was transferred to 10 mL volumetric flask. After appropriate amount of THF was added, water was added dropwise under vigorous stirring to furnish 10 μM mixtures with different water fractions (f_w = 0~90 vol %). The PL measurement of the resultant mixtures were performed immediately.

OLED fabrication. The devices were fabricated by following processes. First, ITO-coated glass substrates were cleaned successively using deionized water, acetone and isopropanol in an ultrasonic bath, and then dried in drying cabinet followed by pretreatment with oxygen plasma. Then the organic films of 1, 4-bis[(1-naphthylphenyl)-amino] biphenyl (NPB), DPATPAN, MeDPATPAN, PhNPATPAN, 8-hydroxyquinoline aluminum salt (Alq_3) and 8-hydroxyquinoline lithium salt (Liq) were deposited by the thermal evaporation under a base vacuum of about 10^{-6} torr. Finally, Al metal was evaporated in another vacuum chamber without breaking the vacuum. The thicknesses of the films were determined by quartz thickness monitors. The active area of the EL device, defined by the overlap of the ITO and the cathode electrode, was 3 mm × 3 mm. Current density-voltage (*J*-*V*) and current efficiency-current density (*CE*-*J*) characteristics were measured with a computer controlled Keithley 2400 Source Meter and BM-7A Luminance Colorimeter. The electroluminescence spectra were measured by Labsphere CDS-610. All measurements were carried out under air at room temperature without device encapsulation.

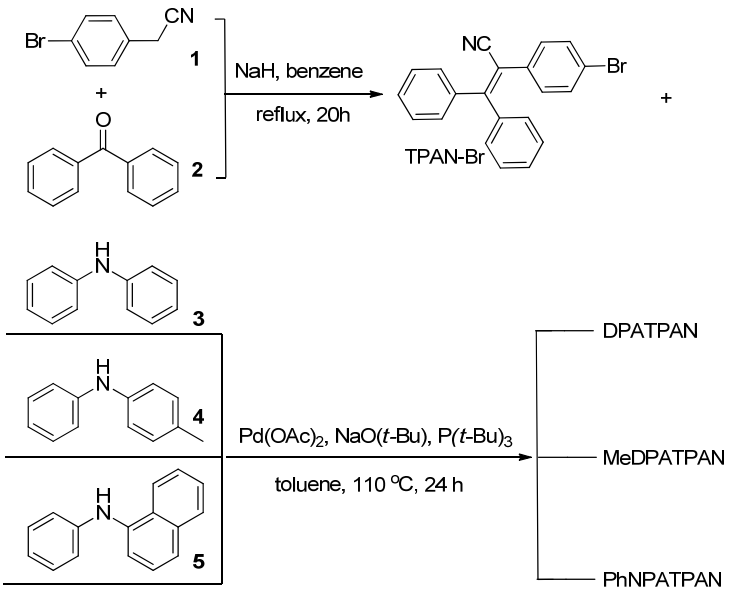

Scheme S1. Synthetic routes to DPATPAN, MeDPATPAN and PhNPATPAN.

Synthesis of 2-(4-bromophenyl)-3,3-diphenylacrylonitrile (TPAN-Br). The compound was synthesized according to the method described in references [1].

Synthesis of 2-(4-(diphenylamino)phenyl)-3,3-diphenylacrylonitrile (DPATPAN). Into a 50 mL two-necked round bottom flask were placed 1.0 mmol (360 mg) TPAN-Br, 1.2 mmol (203 mg) diphenylamine, 134 mg of NaO(*t*-Bu) (1.4mmol), 2 mg $Pd(OAc)_2$ (1% mmol). The flask was evacuated under vacuum and flushed with dry nitrogen three times. And then 20 mL of fresh toluene and 2 mL of P(*t*-Bu)$_3$ (0.5 M in toluene) was injected. The mixtures were refluxed under stirring for 24 h before cooling to room temperature, then diluted with water and extracted with DCM. The combined organic layers were washed with brine, dried over $MgSO_4$, filtered, and condensed by rotary evaporation. The crude product was purification by flash chromatography (silica gel, petroleum ether/DCM ranges from 4/1 to 2/1), affording a light green solid in 83% yield (370 mg). ^{1}H NMR (400 MHz, $CDCl_3$, δ) 7.47-7.38 (m, 5H, Ar-H), 7.26 (m, 7H, Ar-H), 7.11-7.02 (m, 10H, Ar-H), 6.88-6.83 (m, 2H, Ar-H); ^{13}C NMR (100 MHz, $CDCl_3$, δ) 156.18, 148.02, 147.29, 140.88, 139.75, 130.95, 130.76, 130.18, 129.89, 129.60, 129.07, 128.64, 128.48, 128.00, 125.25, 123.83, 122.04, 120.45 (C≡N), 111.57. APCI-MS calcd m/z for $C_{33}H_{24}N_2$: 448.2, Found: 449.5.

Synthesis of 3,3-diphenyl-2-(4-(phenyl(p-tolyl)amino)phenyl)acrylonitrile (MeDPATPAN). The ynthetic procedure for MeDPATPAN is similar to that of DPATPAN described above; a yellow solid

was obtained in 70% yield. ^{1}H NMR (400 MHz, $CDCl_3$, δ) 7.49-7.32 (m, 5H, Ar-H), 7.25-7.15 (m, 5H, Ar-H), 7.13-6.93 (m, 11H), 6.87-6.77 (m, 2H), 2.32 (s, 3H, -CH_3); ^{13}C NMR (100 MHz, $CDCl_3$, δ) 155.92, 148.18, 147.38, 144.65, 140.93, 139.80, 133.90 (*C*-CH_3), 130.93, 130.69, 130.31, 130.18, 129.84(C-H), 129.51, 129.02), 128.62, 128.47, 127.48, 125.82, 124.90), 123.52, 121.40), 120.47 (C≡N), 111.64), 21.12(CH_3). APCI-MS calcd m/z for $C_{34}H_{26}N_2$: 462.2, Found: 463.5.

Synthesis of 2-(4-(naphthalen-1-yl(phenyl)amino)phenyl)-3,3-diphenylacrylonitrile (PhNPATPAN). The Synthetic procedure of PhNPATPAN is similar to that of DPATPAN described above. A light green solid was obtained in 78% yield. ^{1}H NMR (400 MHz, $CDCl_3$, δ) 7.90-7.75 (m, 2H, Ar-H), 7.50-7.35 (m, 8H, Ar-H), 7.32-7.28 (m, 1H, Ar-H), 7.24-7.15(m, 6H, Ar-H), 7.11-6.95 (m, 7H,Ar-H) 6.81-6.73 (m, 2H, Ar-H). ^{13}C NMR (100 MHz, $CDCl_3$) δ 155.86, 148.60, 147.65, 143.02, 140.92, 139.75, 135.48, 131.22, 130.94, 130.74, 130.15, 129.93, 129.81, 129.46, 128.97, 128.69, 128.60, 128.42, 127.50, 127.09, 126.71, 126.53, 126.44, 124.26, 123.30, 123.05, 120.47 (C≡N), 120.06, 111.65. APCI-MS calcd m/z for $C_{37}H_{26}N_2$: 498.2, Found: 499.5.

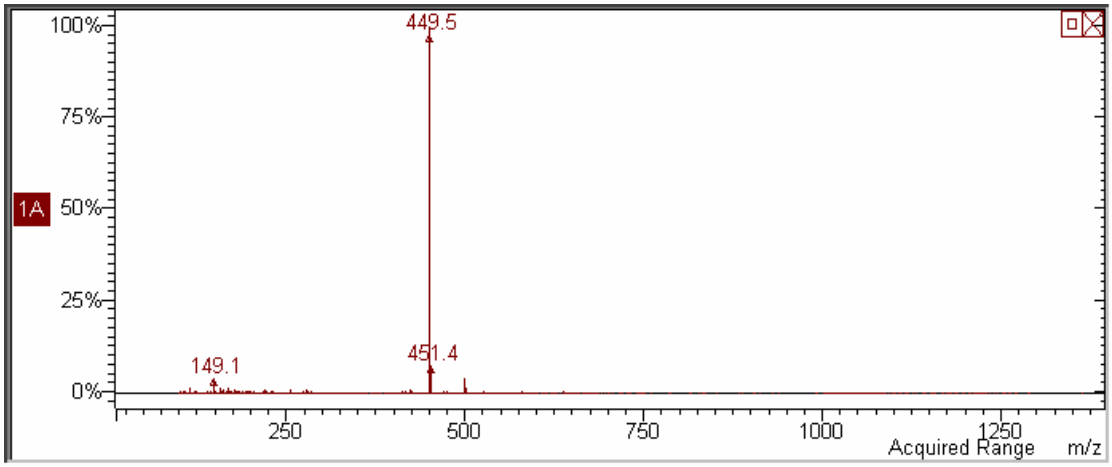

Fig. S1 APCI mass spectrum of DPATPAN.

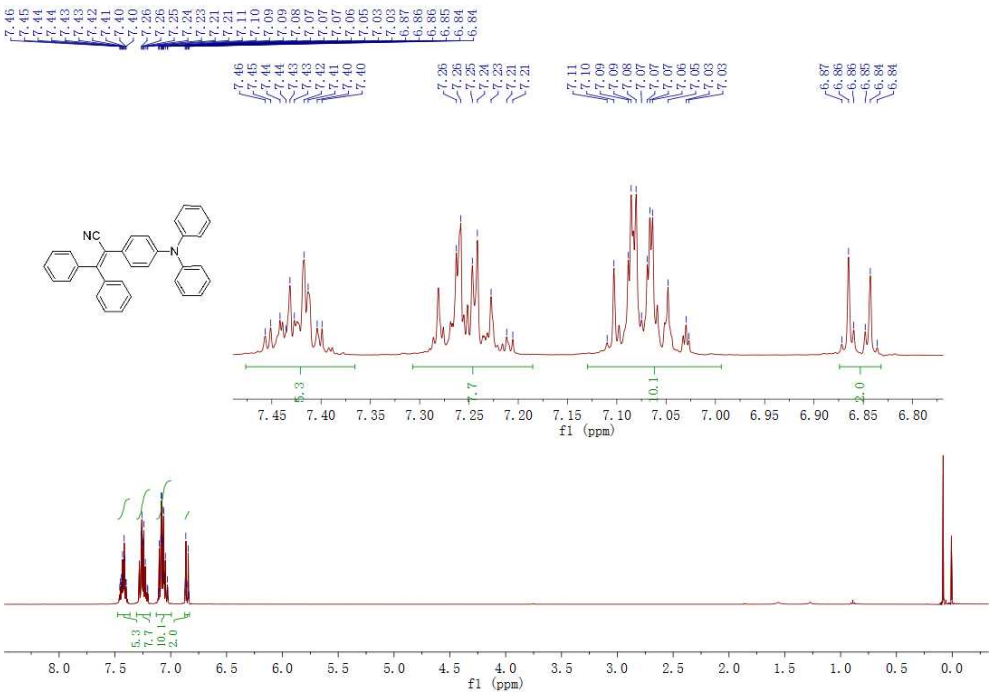

Fig. S2 ^{1}H NMR spectrum of DPATPAN.

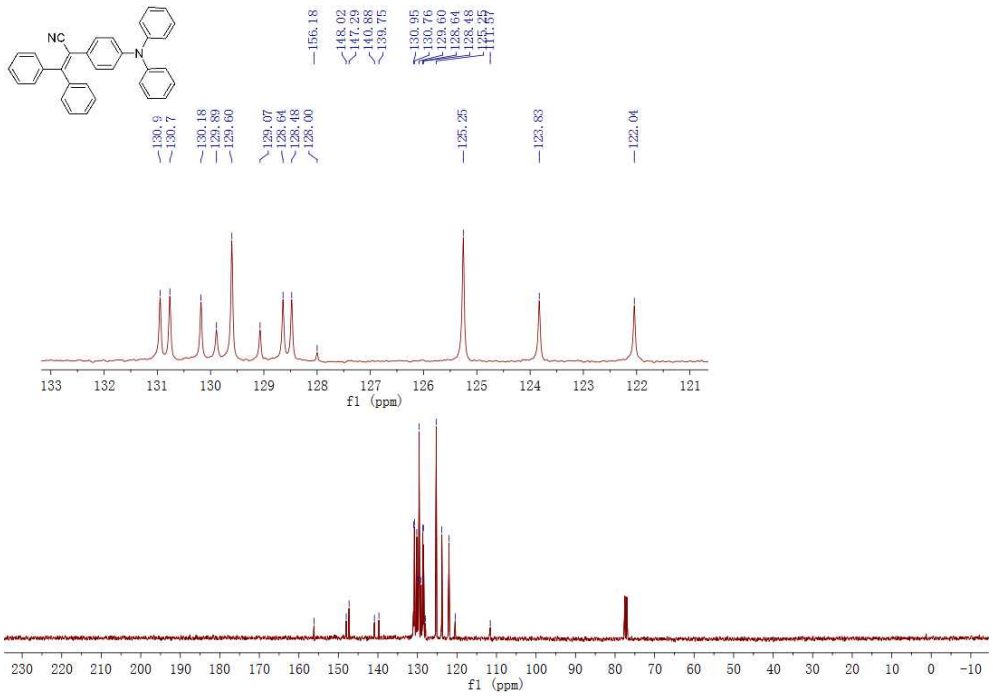

Fig. S3 ^{13}C NMR spectrum of DPATPAN.

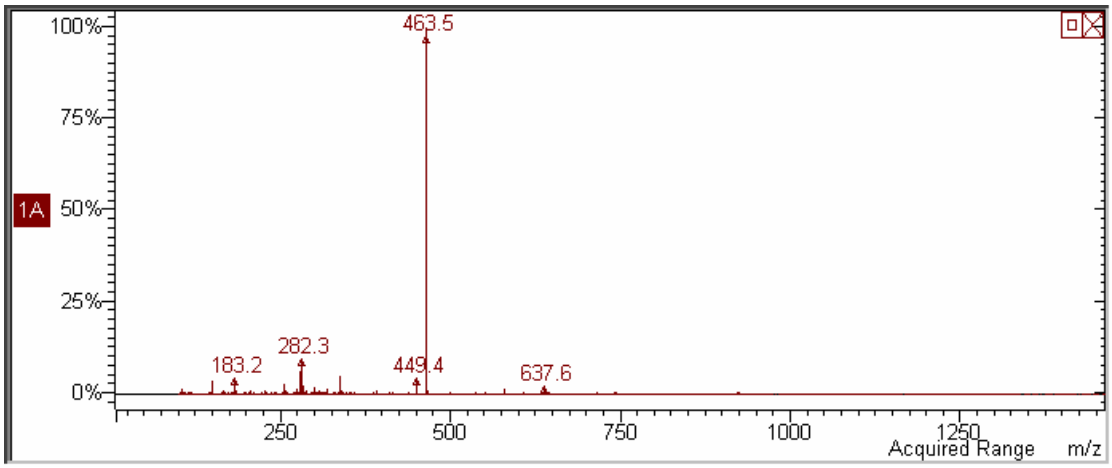

Fig. S4 APCI mass spectrum of MeDPATPAN.

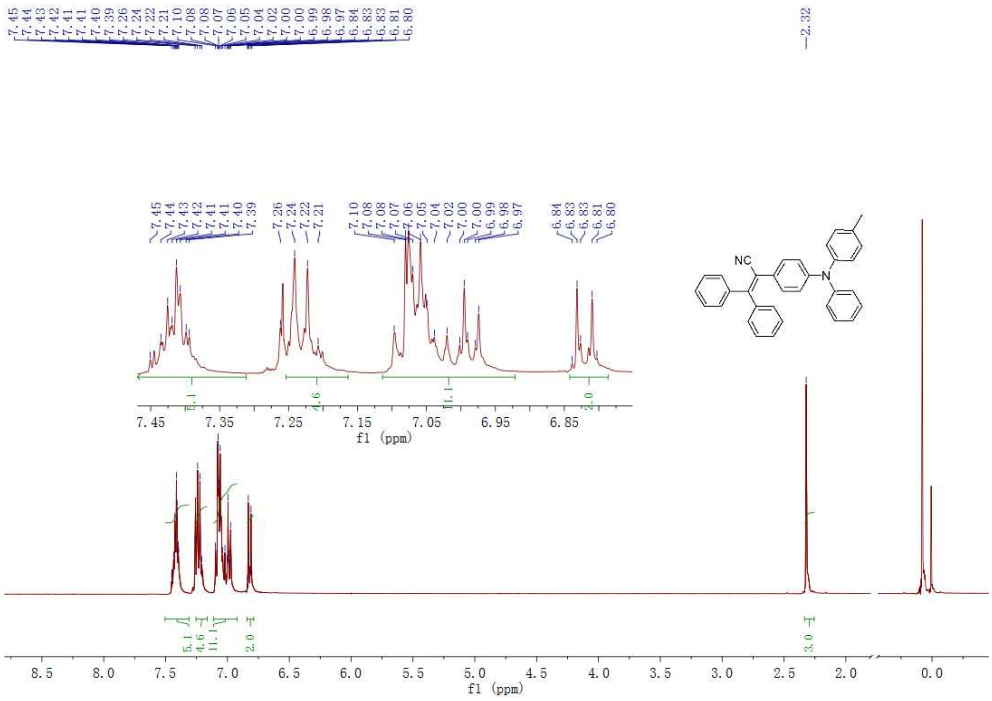

Fig. S5 ^{1}H NMR spectrum of MeDPATPAN.

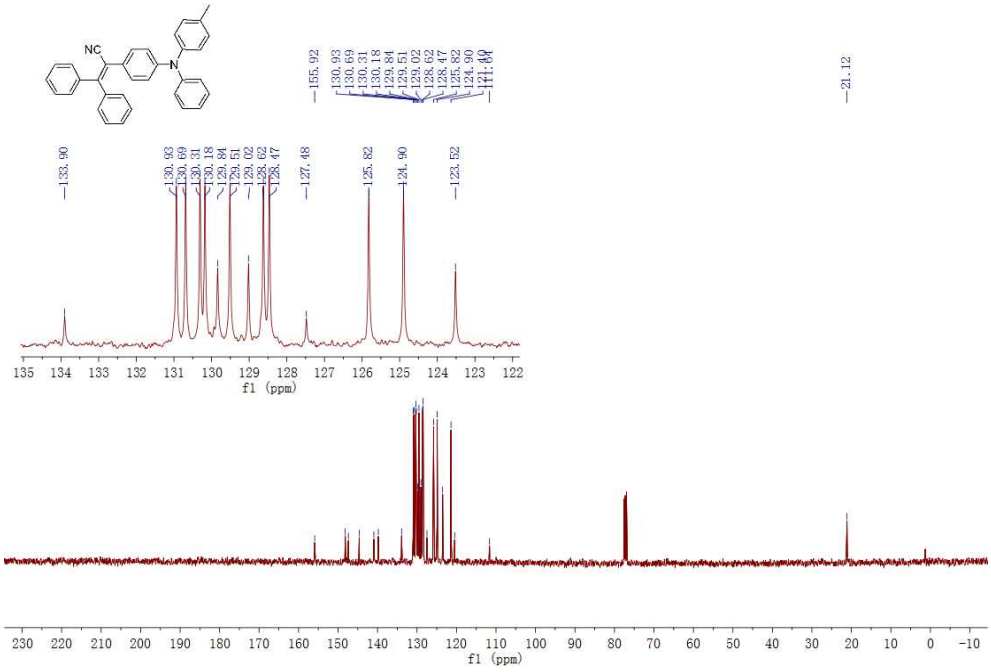

Fig. S6 ^{13}C NMR spectrum of MeDPATPAN.

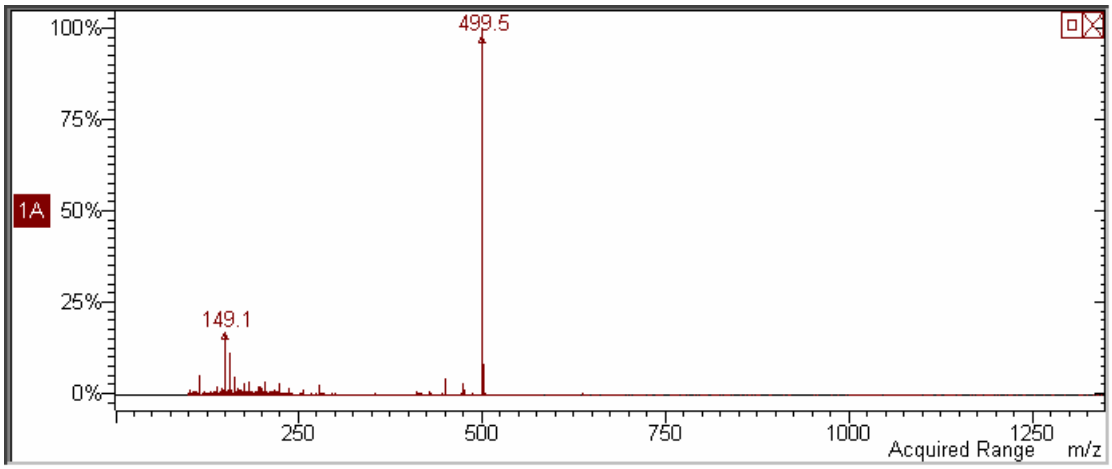

Fig. S7 APCI mass spectrum of PhNPATPAN.

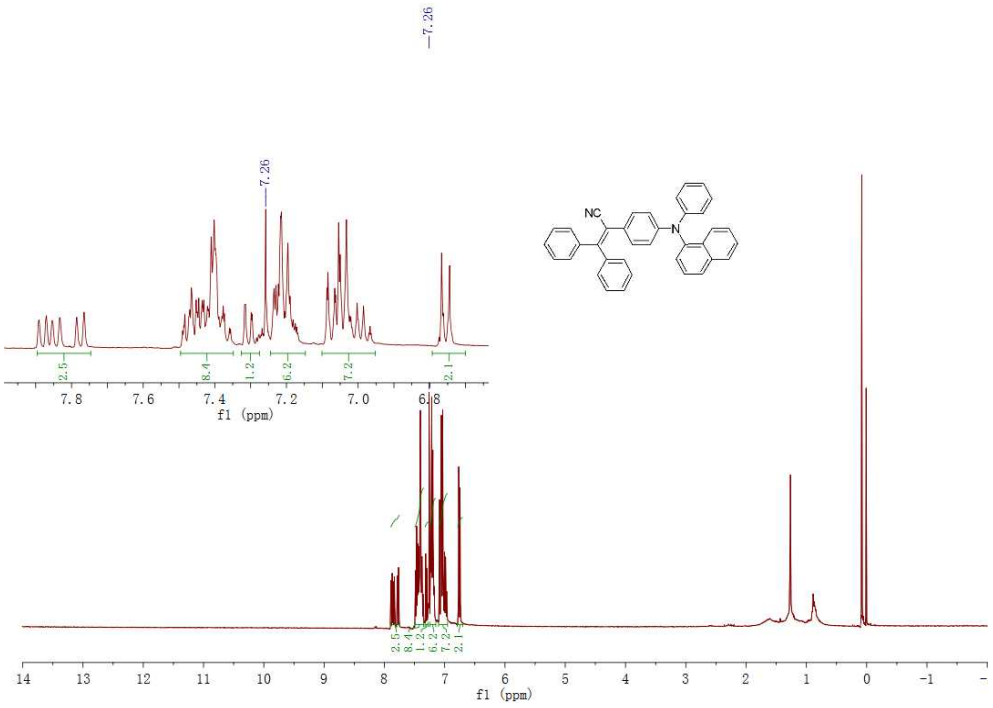

Fig. S8 ^{1}H NMR spectrum of PhNPATPAN.

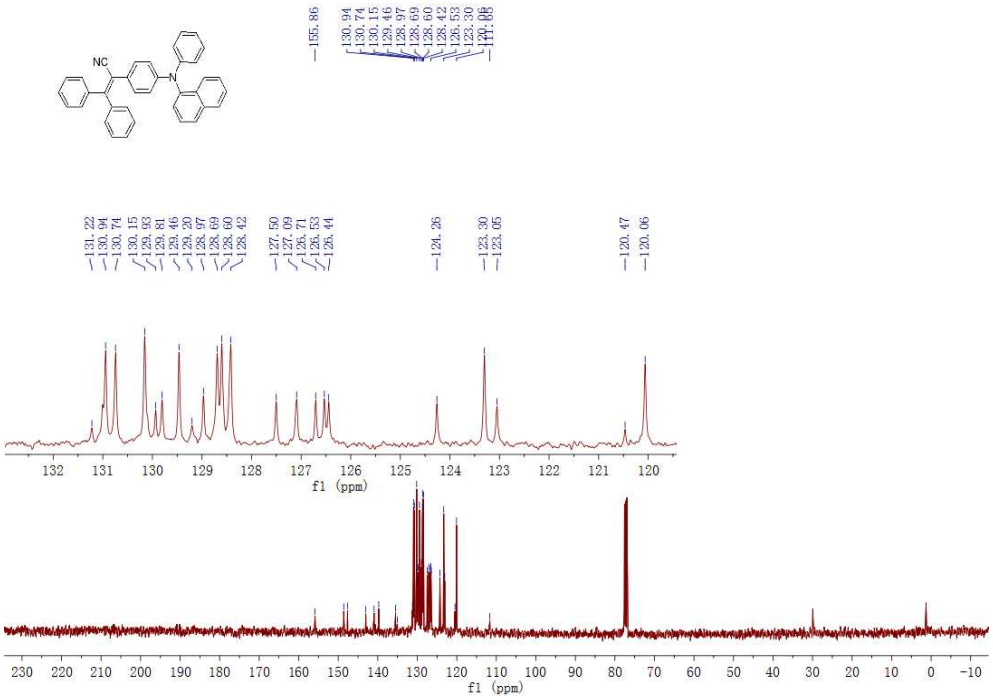

Fig. S9 ^{13}C NMR spectrum of PhNPATPAN.

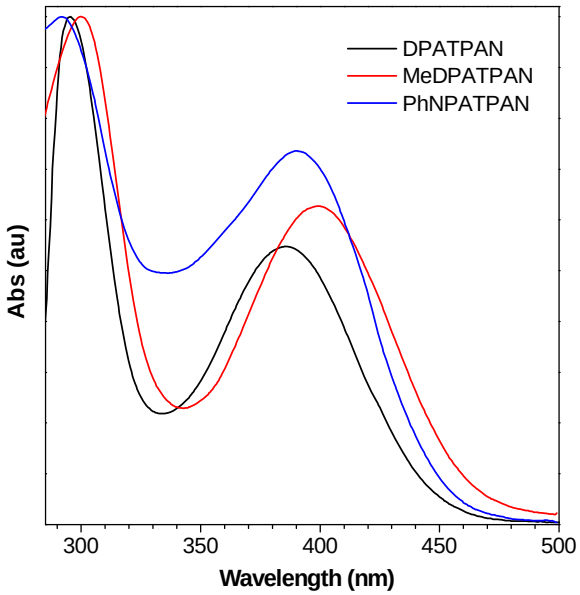

Fig. S10 Normalized absorption spectra of DPATPAN, MeDPATPAN and PhNPATPAN in THF.

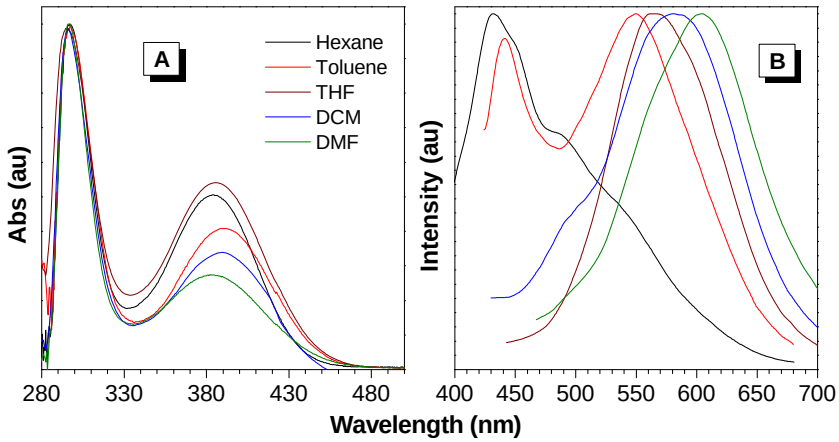

Fig. S11 Normalized (A) absorption and (B) emission spectra of DPATPAN in varying solvents. Excitation wavelength = 380 nm. Concentration: 20 μM.

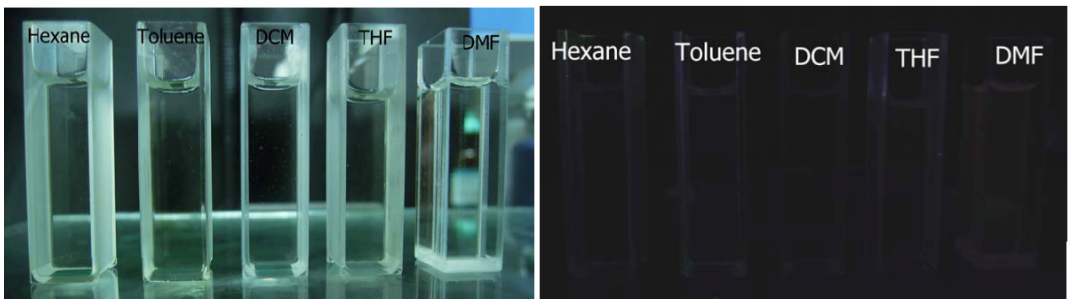

Fig. S12 Photographs of DPATPAN in different solvents under (left) room light and (right) 365-nm UV light illumination. Concentration: 20 μM.

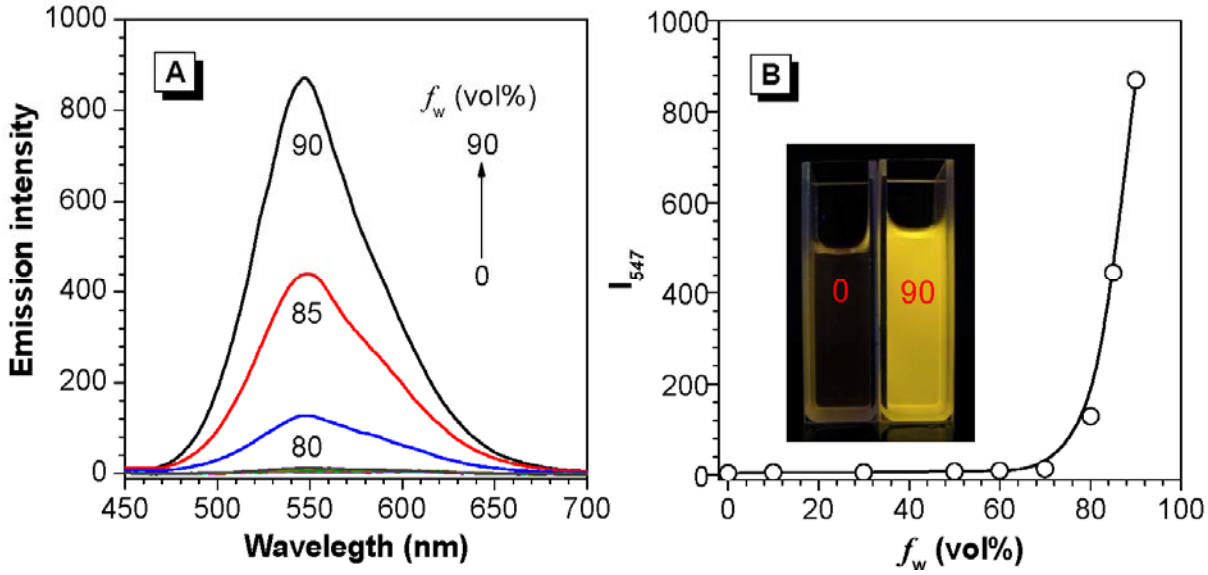

Fig. S13 (A) PL spectra of MeDPATPAN in THF and THF/water mixtures with varying water fractions (f_w). (B) Plot of PL intensity of MeDPATPAN at 547 nm *vs* f_w. Concentration: 10 μM; excitation wavelength: 400 nm. Photographs in (B) are MeDPATPAN in THF and 10/90 THF/water mixture taken under 365-nm UV light illumination.

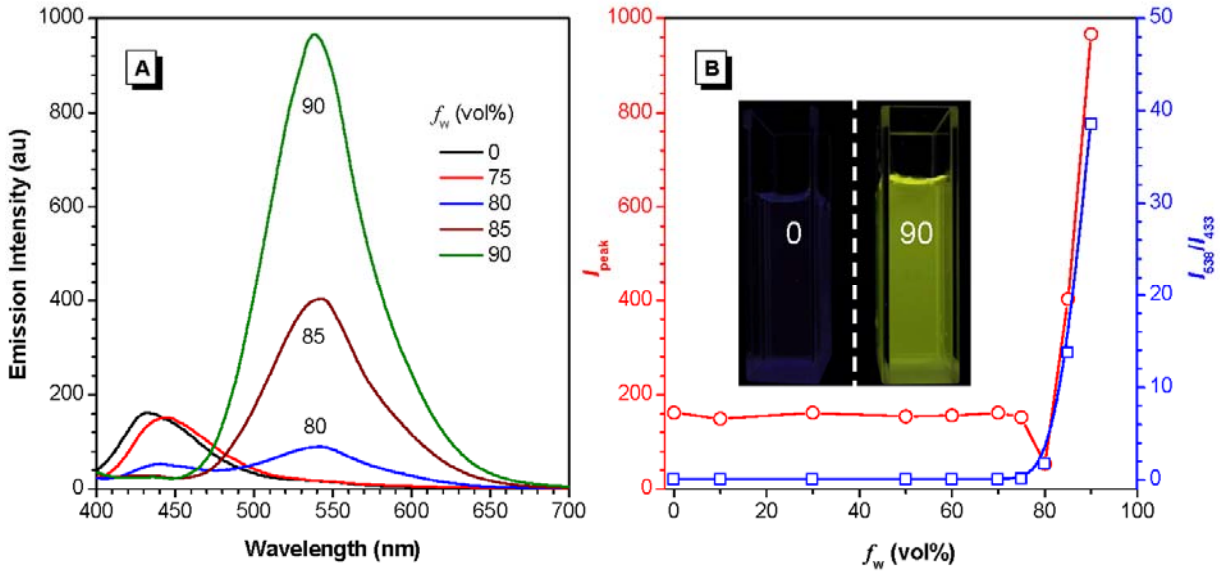

Fig. S14 (A) PL spectra of PhNPATPAN in THF and THF/water mixtures with varying water fractions (f_w). (B) Plot of PL peak intensity of PhNPATPAN *vs* f_w. Concentration: 10 μM; excitation wavelength: 400 nm. Photographs in (B) are PhNPATPAN in THF and 10/90 THF/water mixture taken under 365-nm UV light illumination.

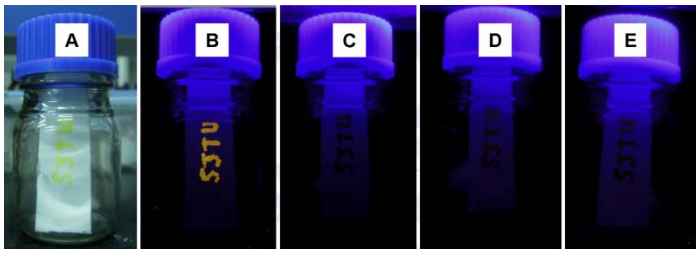

Fig. S15 Photographs of DPATPAN dotted on a TLC plate placed in air under (A) room light and (B) 365-nm UV light and in (C) DCM, (D) chloroform, and (E) THF vapors under 365-nm UV light irradiation.

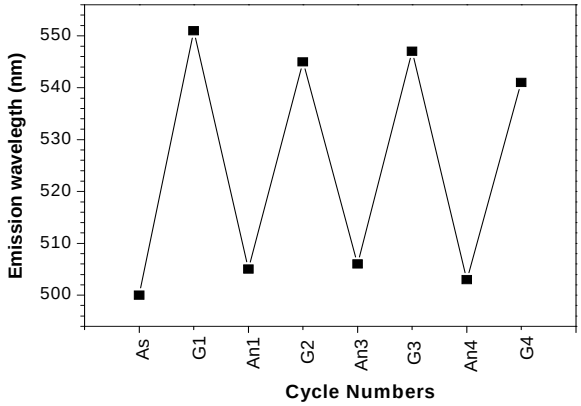

Fig. S16 Emission maxima of DPATPAN during the grinding-heating cycles. As = as prepared sample, G = ground sample; An = annealed sample (annealed at 80 ^{o}C for 10 min). The numbers after G or An represent cycle numbers.

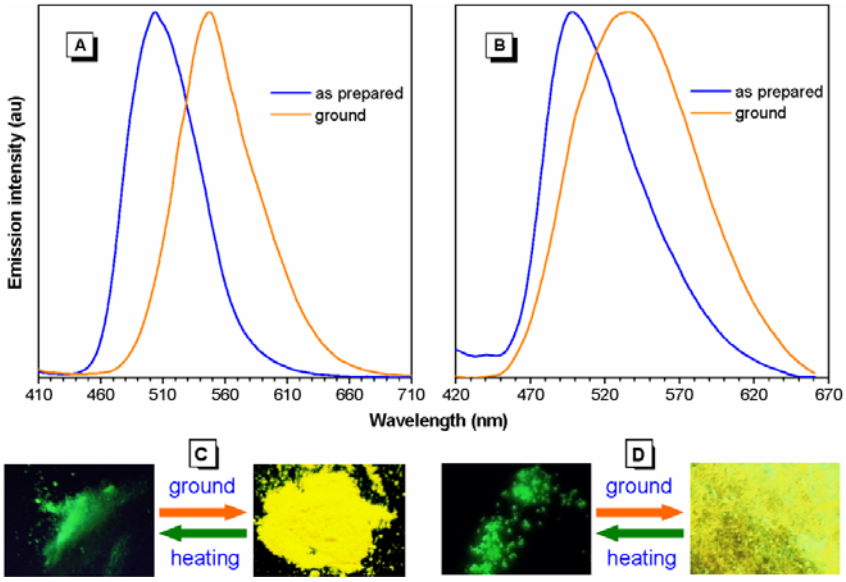

Fig. S17 (A, B) Emission spectra and (C, D) photographs (under 365-nm UV light irradiation) of as prepared and ground solids for (A, C) MeDPATPAN and (B, D) PhNPATPAN, respectively.

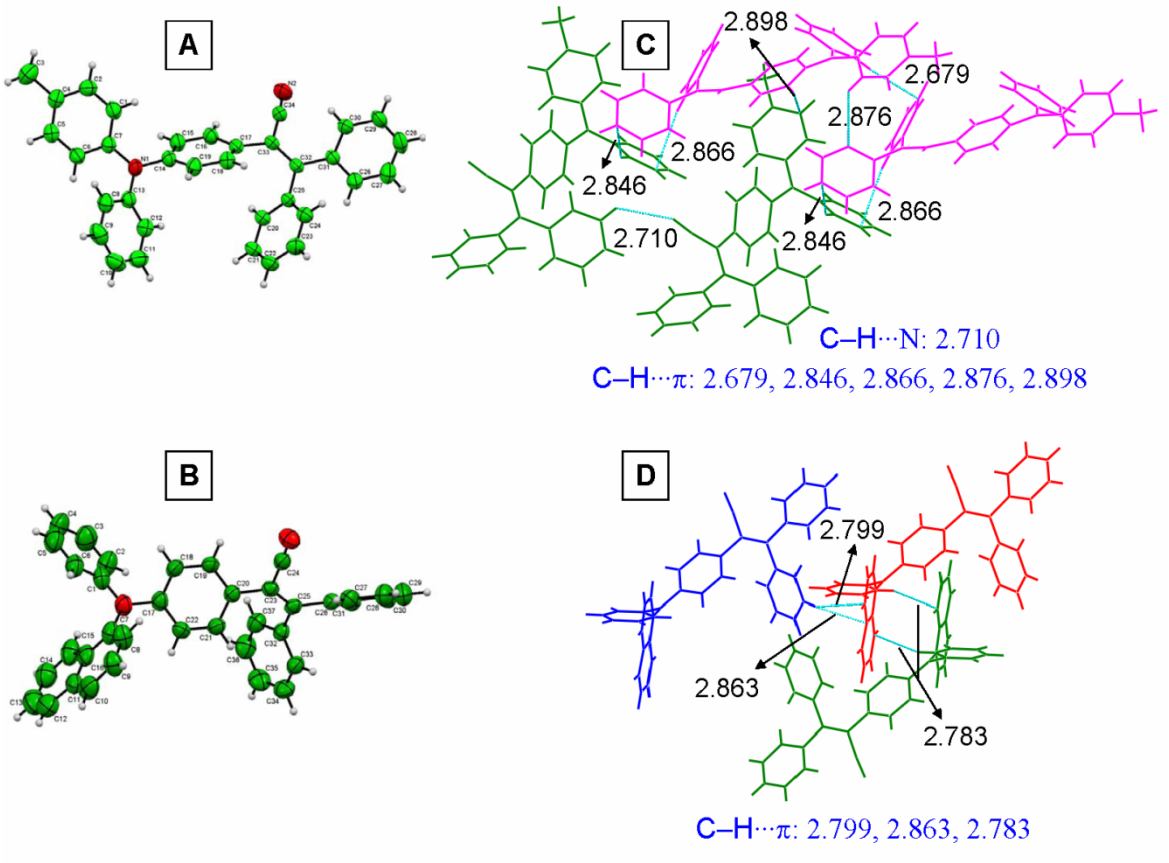

Fig. S18 (A, B) ORTEP drawing and (C, D) molecular packing of the crystals for (A, C) MeDPATPAN and (B, D) PhNPATPAN, respectively. Exampled C−H···N and C−H···π intermolecular interactions are depicted in B and D.

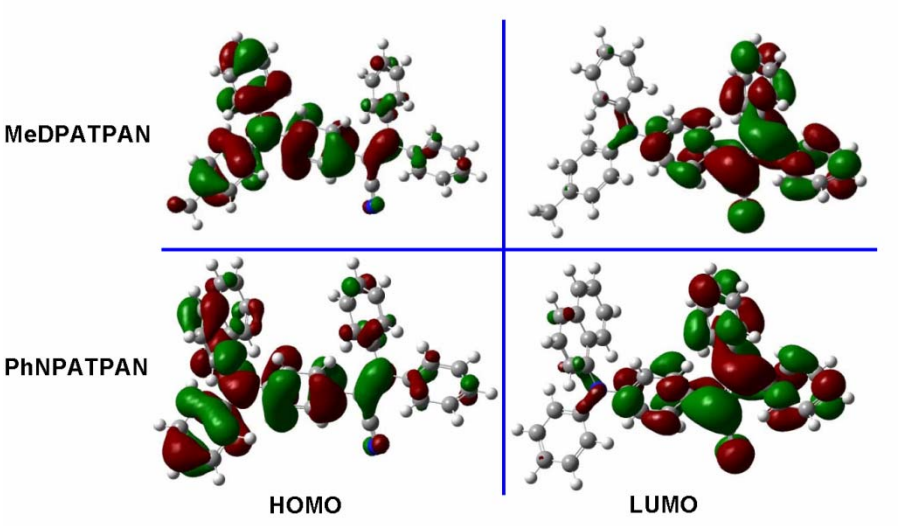

Fig. S19 B3LYP/6-31G(d) calculated molecular orbital amplitude plots of HOMO and LUMO levels for MeDPATPAN and PhNPATPAN.

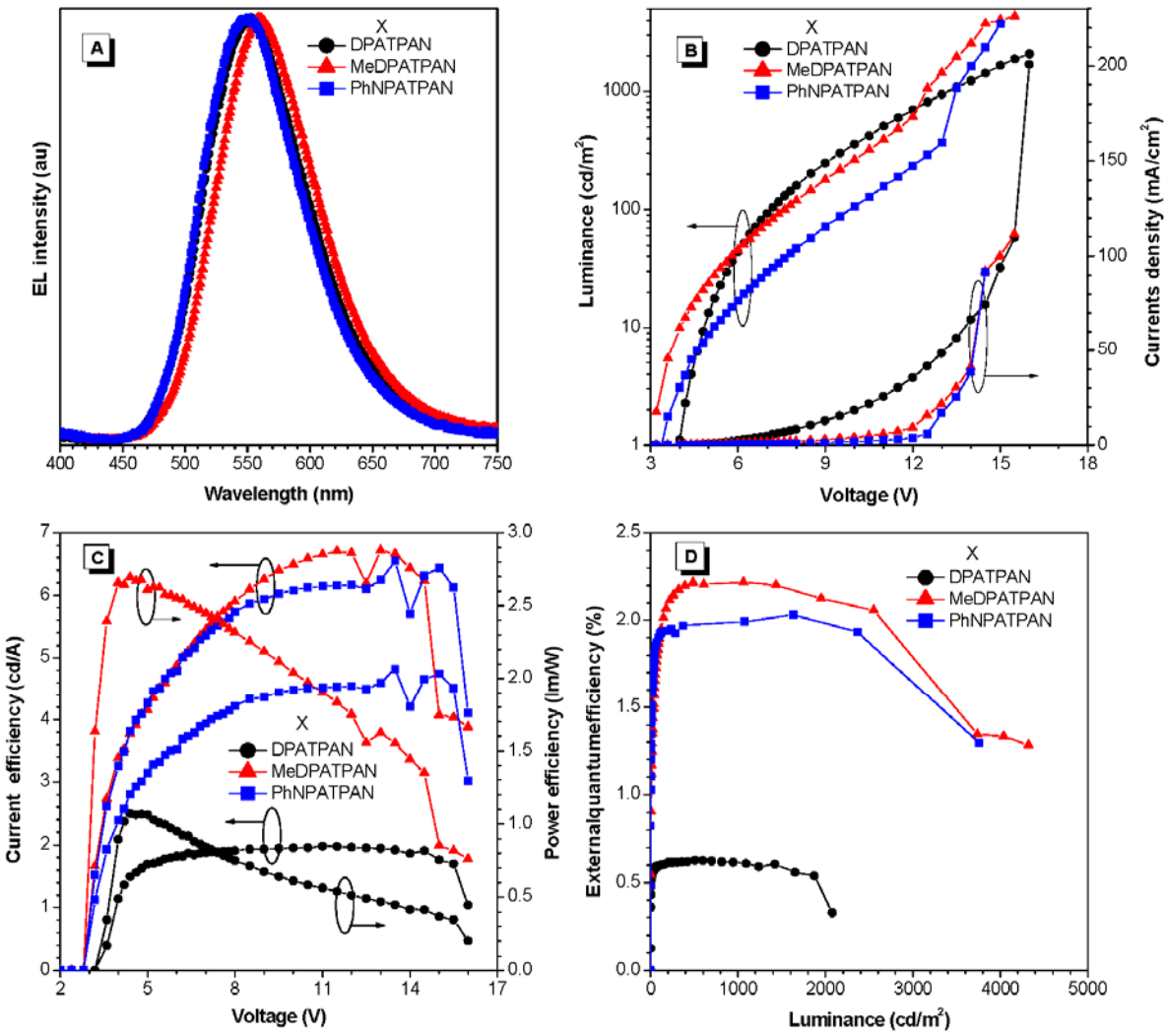

Fig. S20 (A) EL spectra of DPATPAN, MeDPATPAN and PhNPATPAN with the device configuration of ITO/NPB (60 nm)/X (30 nm)/Alq_3 (30 nm)/Liq (1 nm)/Al (150 nm), (B) plots of luminance-voltage-current density, (C) plots of current efficiency and power efficiency *versus* driving voltage of the devices, and (D) external quantum efficiency as a function of the luminance.

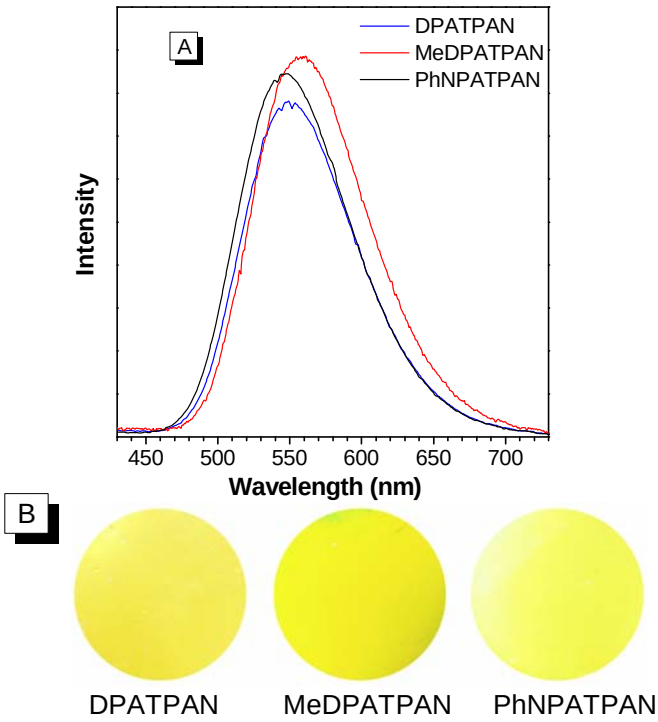

Fig. S21 (A) Emission spectra of vacuum deposited thin films of DPATPAN, MeDPATPAN andPhNPATPAN and (B) their photographs taken under 365-nm UV light illumination.

References

(1) (a) S. Wang, W. J. Oldham, Jr., R. A. Hudack, Jr., G. C. Bazan, *J. Am. Chem. Soc*., 2000, **122**, 5695; (b) W. Z. Yuan, Y. Gong, S. Chen, X. Y. Shen, J. W. Y. Lam, P. Lu, Y. Lu, Z. Wang, R. Hu, N. Xie, H. S. Kowk, Y. Zhang, J. Z. Sun and B. Z. Tang, *Chem. Mater.*, 2012, **24**, 1518.